

Astron. Astrophys. Suppl. Ser. **64**, 439-451 (1986)

Supernova matter : a semiclassical approach

M. Pi ⁽¹⁾, X. Viñas ⁽¹⁾, M. Barranco ⁽¹⁾, A. Perez-Canyellas ⁽²⁾ and A. Polls ⁽¹⁾⁽¹⁾ Física Atòmica i Nuclear, Facultat de Física, Universitat de Barcelona, Diagonal 645, 08028 Barcelona, Spain⁽²⁾ Física Teòrica, Facultat de Física, Universitat de València, Burjassot (València), Spain

Received February 4, accepted September 3, 1985

Summary. — We have used a well established semiclassical method to study systematically the properties of hot dense matter in the conditions prevailing during the gravitational collapse of massive stars. Different semiclassical kinetic energy and entropy densities are discussed. Detailed results for different nuclear forces having different nucleon effective mass m^* and nuclear incompressibility K are presented. Plasma effects (translational and vibrational energies and Coulomb excess) are considered for a typical adiabat. The results here presented cover a wide range in entropy per baryon S/A and electron concentration per baryon Y_e for baryon densities ρ_B ranging from 10^{-3} fm^{-3} to 0.30 fm^{-3} .

Key words : stellar evolution — supernova theory — equation of state.

1. Introduction.

In recent years, a considerable effort has been devoted to the study of hot dense matter (see Lamb *et al.*, 1984 for an exhaustive review of the literature). Besides its fundamental importance for the collapse of massive stars, the study of matter under such extreme conditions is interesting by itself. Indeed, it has been found that due to the effect of the Coulomb lattice energy, cold matter near the nuclear matter (NM) saturation density may adopt exotic configurations (Ravenhall *et al.*, 1983; Hashimoto *et al.*, 1984; Oyamatsu *et al.*, 1984; Williams and Koonin, 1985). The search of a liquid-gas phase transition in heavy ion reactions is another related topic of growing interest nowadays (Siemens, 1984 and references therein).

Within the equation of state (EOS) context, several groups have undertaken its study using methods of different accuracy and complexity. Since the pioneering work of Lamb *et al.* (1978) using a finite temperature (T) Compressible Liquid Drop (CLD) model (Lamb *et al.*, 1984), complementary results from other groups have become available. Mazurek *et al.* (1979) and El Eid and Hillebrandt (1980) described hot dense matter as a statistical equilibrium between different nuclei. This approximation breaks down at densities $\rho_B \gtrsim 0.01 \text{ fm}^{-3}$ when the external neutron gas starts being sizeable. Barranco and Buchler (1981) and Marcos *et al.* (1982) used a $T \neq 0$ Energy Density (Thomas-Fermi (TF)) method with trial functions as nuclear densities. Later on, fully variational TF calculations were performed by Ogasawara and Sato (1983), Suraud and Vautherin (1984) and Ogasawara (1985).

At present, the more reliable EOS results come from spherical Thermal Hartree-Fock (THF) calculations (Bonche and Vautherin, 1981; 1982; Hillebrandt *et al.*, 1984). Also non spherical THF calculations have been performed (Wolff, 1983), but no detailed results are yet available. The main shortcoming of THF calculations is that they are extremely time consuming. Moreover, in the range of densities and temperatures we are interested in, shell effects are completely washed out and thus HF calculations do not seem necessary at all. Nevertheless, they are very useful as a test for faster and cheaper semiclassical methods.

It is the aim of this work to present a rather detailed EOS calculated with a semiclassical TF method free from most of the drawbacks TF methods are often criticized for in the literature. We have also checked the influence of different available approximations to the kinetic energy density (KED) on quantities relevant for the EOS (entropy, T , pressure, etc.). For isolated nuclei, the choice of the KED is crucial but we anticipate that the EOS turns out to be rather insensitive to that choice. Since in the regime where nuclear clusters exist, the gross features of the EOS are essentially determined by the leptons, provided the model used to obtain the EOS is able to find these clusters at the right T and ρ_B , no dramatic changes are expected in the results obtained from different methods. This is the ultimate reason why CLD, TF and HF calculations yield similar results.

At the beginning of this work, it was also our aim to present the results at $T = 0$ and at finite temperature corresponding to finite nuclei and semi-infinite NM as well, showing the capabilities of a method that might be useful for a wide variety of problems. However, two

Send offprint requests to : M. Barranco.

complete recent papers by Brack and coworkers (Brack, 1983; Brack *et al.*, 1984) make unnecessary that part of our work. We refer the interested reader to these two references for an exhaustive and especially clear description of the so-called Extended-TF (ETF) method and its achievements.

The plan of this paper is as follows. We present the Thermal ETF (TETF) method in section 2. Some details about our minimization procedure are given in section 3. The results are presented in section 4. Plasma effects are discussed in section 5 and a short discussion about alpha particles is given in section 6. Finally, section 7 contains our conclusions. Part of this work has been presented elsewhere (Viñas *et al.*, 1984; Barranco *et al.*, 1984).

2. The TETF method.

Since a complete description of the method has been given by Brack *et al.* (Brack, 1983; Brack *et al.*, 1984), we present here only a brief outline of the procedure.

The starting point is the free energy density which for Skyrme-like forces is written as follows :

$$\mathcal{F}[\rho_n, \rho_p, \tau_n, \tau_p] = \mathcal{H}[\rho_n, \rho_p, \tau_n, \tau_p] - T \sum_q S_q(\rho_q, \tau_q) \quad (1)$$

$\mathcal{H}[\rho_n, \rho_p, \tau_n, \tau_p]$ is a zero temperature Hamiltonian density depending on the particle and kinetic energy densities ρ_q and τ_q . Its general expression can be found in the work of Rayet *et al.* (1982). Within the Thomas-Fermi approximation, the entropy density reads

$$S_q = \frac{5}{3} \frac{\hbar^2}{2 m_q^*} \tau_q - \rho_q \eta_q \quad (2)$$

where m^* is the local nucleon effective mass and η_q is the degeneracy parameter

$$\eta_q = \frac{1}{T} (\mu_q - V_q). \quad (3)$$

V_q is the single particle potential and μ_q the chemical potential.

As it is obvious from equation 1, the two key ingredients entering the definition of \mathcal{F} are the Hamiltonian density \mathcal{H} and (for semiclassical calculations) the KED τ_q . Since no attention has been paid until now to the influence of both quantities on EOS calculations (see however Viñas *et al.*, 1981; Rayet *et al.*, 1982 and Hartmann *et al.*, 1984), it is worth discussing first the properties one should ask \mathcal{H} to bear in order to be reliable for EOS computations.

2.1 THE HAMILTONIAN DENSITY. — We will limit our analysis to Skyrme-like forces (Beiner *et al.*, 1975; Tondeur *et al.*, 1984) because all the EOS calculations are (and have been) performed with that kind of interactions.

It is quite obvious that the Hamiltonian density should reproduce correctly the average binding energy of terrestrial nuclei. This is the case for all effective Hamiltonians so far used in EOS calculations. (Actually, the SkM force used by Bonche and Vautherin (1981; 1982) slightly overbinds; see Bartel *et al.*, 1982.) Moreover, it should be reliable for the description of neutron-rich nuclei and

should reproduce fairly well the neutron matter properties (energy per nucleon and chemical potential) computed with realistic nuclear forces (Friedman and Pandharipande, 1981). In this respect, only the forces used by Barranco and Buchler (1981); Lamb *et al.* (1978) and the RATP force of Rayet *et al.* (1982) were built so as to take into account the properties of the neutron gas. The forces SkM and SkM* were constructed without paying any attention to the neutron gas and their symmetry properties need to be ameliorated (Brack *et al.*, 1984).

The influence of the symmetry properties of the force on the final results is masked by other bigger contributions to the EOS. There are two characteristics of the force relevant enough to yield significantly different EOS. These are the nuclear incompressibility K and the nucleon effective mass m^* . Let us show in a simple way their influence on the final results.

For the sake of explicitness, we consider homogeneous, symmetric NM. For Skyrme-like forces, the Hamiltonian density reads

$$\mathcal{H}(\rho, \tau) = \frac{\hbar^2}{2 m^*} \tau + P(\rho) \quad (4)$$

where $P(\rho)$ is a sum of powers of ρ . When the nuclear clusters merge into homogeneous high density NM, it is the highest ρ -power in $P(\rho)$ that determines the adiabatic index γ .

$$\gamma = \left(\frac{\partial \log P}{\partial \log \rho} \right)_s. \quad (5)$$

It turns out that the nuclear incompressibility is also determined by that ρ -power (Bohigas *et al.*, 1979). For old Skyrme forces with $K \sim 350$ MeV like the one used by Lamb *et al.* (1978, 1984), one has $P(\rho) \sim \rho^3$ and thus $\gamma \sim 3$ whereas for forces having reasonable values of K (~ 220 MeV), one has $P(\rho) \sim \rho^{2+\delta}$ with $\delta = 1/3$ or $1/6$ and consequently $\gamma \sim 2$. The unrealistic high value of K does not seem to be of crucial importance up to the point where nuclear clusters disappear because the pressure is essentially determined by the leptons and $\gamma \sim 4/3$. However, this is quite not so beyond that point. It is worth noting that at temperatures as low as 4 MeV and $Y_e \sim 0.30$, the system becomes homogeneous at a rather low density ($\rho \sim 0.10 \text{ fm}^{-3}$). Consequently, forces with high K will procedure an unacceptable artificial stiffening of the EOS and should be avoided in EOS calculations.

The nucleon effective mass m^* plays an important role in determining the nucleon single particle (s.p.) spectrum, more precisely, the s.p. level density near the Fermi surface (Brown *et al.*, 1962; Jeukenne *et al.*, 1976). This level density is crucial for the nuclear thermal properties.

An effective mass $m^*/m \sim 0.80$ for homogeneous symmetric NM seems to stem from the systematics of giant monopole and quadrupole isoscalar resonances (Bohigas *et al.*, 1979; Krivine *et al.*, 1980). However, a value $m^*/m \sim 1$ is needed to reproduce the level density near the Fermi surface and might be an approximate way to incorporate collective effects in HF which are in part responsible of the enhancement of m^*/m . We may expect these effects still to remain at moderate T making $m^*/m \sim 1$ more likely, whereas at high T the collective effects will be washed out and 0.80 would be probably more adequate.

Just to give a crude estimate on the effect of m^* on the EOS, let us consider again symmetric homogeneous NM at low T . The relationship between the entropy per particle S/A and T is (Barranco and Treiner, 1981)

$$\frac{S}{A} = \frac{\pi^2}{\hbar^2 k_F^2} m^* T \quad (6)$$

where $\hbar k_F$ is the Fermi momentum. Thus, for a given value of S/A , the corresponding value of T may vary by as much as 20%. The variation is less dramatic when electrons and surface effects are taken into account, but it may still be a sizeable 10% (Hartmann *et al.*, 1984). Any further discussion of this point is beyond our scope. However, full EOS calculations are desirable in order to have a precise idea of the influence of m^* on the results.

Having in mind this discussion, we have chosen for our calculations the T6 interaction of Tondeur *et al.* (1984). This force has several interesting features. First, it has already been used in the astrophysical context (Rayet *et al.*, 1982). It has $m^*/m = 1$ and reproduces the nuclear binding energies accurately (Tondeur *et al.*, 1984). Its symmetry properties are also excellent, reproducing correctly the results of Friedman and Pandharipande (1981) and the so-called « neutron skin » in ^{208}Pb . It is thus reliable for the study of neutron-rich nuclei. Its correct incompressibility (~ 240 MeV) also ensures a good behaviour of the EOS at high density.

A common feature of all EOS Thomas-Fermi calculations performed up to now is the neglecting of the spin-orbit (SO) energy density entering the definition of \mathcal{H} . Although its contribution to the total nuclear energy may not be very relevant, the SO energy accounts for 5-10% of the surface energy (Negele and Vautherin, 1975; Côté and Pearson, 1978; Grammaticos and Voros, 1980). Because the nuclear size is determined by a critical balance between surface and Coulomb energies, one may expect the same variation in the nuclear size if the SO force is not included and the surface energy is not readjusted. Actually, the nuclear size uncertainty due to thermal fluctuations is bigger than 10% (Barranco and Buchler, 1981; Bonche and Vautherin, 1982; Hartmann *et al.*, 1984). We want to point out that it is straightforward to include the semiclassical SO force in the calculations, avoiding any sort of *ad hoc* renormalization of the surface free energy. (This renormalization is around 20% in the CLD model but is not only due to the neglecting of the SO force.) Consequently, we have used the full expression of the T6 Hamiltonian density except the terms proportional to the square of the spin-orbit density \mathbf{J} because this is also usually done in HF calculations.

2.2 THE KINETIC ENERGY DENSITY. — Another key ingredient entering the (semiclassical) definition of \mathcal{F} is the kinetic energy density τ_q . For isolated nuclei at zero temperature, it is well known that one has to go beyond the standard $\rho_q^{5/3}$ term in order to get variational densities ρ_q valid all over the space (Lombard, 1973; Bohigas *et al.*, 1976). The inclusion of the so-called Weiszäcker term $(\nabla\rho_q)^2/36\rho_q$ allows to obtain nuclear densities with an exponential fall-off, but too steep at the surface. This can be cured by an *ad hoc* reduction of the Weiszäcker term coefficient but in this case the price one pays for having

a good nuclear surface is the losing of ~ 0.5 MeV/nucleon binding energy. In other words, it is beyond any hope to have a good surface and the correct binding energy at the same time.

It seems that the only way to obtain the correct binding energy and surface diffuseness *simultaneously* is to go to higher orders in the semiclassical expansion of τ_q in terms of ρ_q and its gradients. This expansion has been obtained by Grammaticos and Voros (1980) and successfully applied by M. Brack *et al.* (see Brack *et al.*, 1984 and references therein) to the study of static and dynamic nuclear properties. We refer the interested reader to that reference where one may find exhaustive comparisons between HF and semiclassical results at zero and finite T . These calculations are not fully variational in the sense that instead of solving the Euler-Lagrange equations as Bohigas *et al.* (1976) did, the nuclear densities were parametrized Fermi-like functions. The total energy is minimized with respect to the density parameters and the agreement with HF calculations turns out to be excellent.

One of the nicest features of the complete functional $\tau_q[\rho_q]$ is that it includes contributions coming from non-local effects (i.e., nucleon effective mass and spin-orbit energy). Consequently, besides including higher term in $\tau_q[\rho_q]$ that take account of the inhomogeneities, one is able to handle nuclear forces having effective mass and to incorporate the spin-orbit density in the semiclassical calculation. Moreover, this procedure is completely free of any adjustable parameter. Once the nuclear Hamiltonian has been chosen, the associated functional $\tau_q[\rho_q]$ is unique (Grammaticos and Voros, 1980).

At finite temperature, the procedure we have followed to generalize the $T = 0$ results is the following. We write the KED as a sum of three terms

$$\begin{aligned} \tau_q &= \frac{1}{2\pi^2} \left(\frac{2m_q^* T}{\hbar^2} \right)^{5/2} J_{3/2}(\eta_q) + \tau_{2q} + \tau_{4q} \equiv \\ &\equiv \tau_q^v + \tau_{2q} + \tau_{4q}. \end{aligned} \quad (7)$$

The corrective terms τ_{2q} and τ_{4q} are the *cold* second and fourth order ones (Grammaticos and Voros, 1980). $J_{3/2}$ is the Fermi integral

$$J_\nu(\eta) \equiv \int_0^\infty \frac{x^\nu dx}{1 + \exp(x - \eta)}. \quad (8)$$

Equation (7) together with the standard definition of ρ_q

$$\rho_q = \frac{1}{2\pi^2} \left(\frac{2m_q^* T}{\hbar^2} \right)^{3/2} J_{1/2}(\eta_q) \quad (9)$$

define implicitly the functional $\tau_q[\rho_q]$.

We want to stress that the terms τ_{2q} and τ_{4q} do not depend explicitly on T but will change with it due to the changes produced in the mean field by the temperature. For the entropy per unit volume we take equation (2) with τ_q^v instead of τ_q (Barranco and Treiner, 1981).

During the completion of this work, we became aware that M. Brack had worked out the exact finite temperature second order term τ_{2q}^v (Brack, 1984). This correction implies also an extra gradient term in the definition of s that may play some role at low temperature ($\lesssim 3$ MeV)

but which is not relevant at higher T , as we have checked (see also Brack, 1984). We will come back to this point when we discuss the results.

To work out the corrective terms τ_{2q} and τ_{4q} is a rather cumbersome task. Their explicit expression can be found in Brack *et al.* (1984). We want to point out that we have derived them independently as well as the computer code for isolated nuclei at $\mathbf{T} = 0$ and finite T . Consequently, we have been able to check extensively the results given in that reference. In no case we have found any appreciable disagreement⁽¹⁾.

3. Minimization procedure.

To obtain the thermodynamical properties of a system of nucleons, electrons and neutrinos (other particles are extremely rare in the range of temperature and density in which we are interested) we minimize the free energy per unit volume

$$\frac{F}{V}[\rho_n, \rho_p, \tau_n, \tau_p, T] = \frac{1}{V} \int d\mathbf{r} \left[\mathcal{F}_{\text{nuc}}(\bar{r}) + \frac{1}{2} e(\rho_p - \rho_e) \Phi_{\text{coul}}(\bar{r}) - \frac{3}{4} \left(\frac{3}{\pi}\right)^{1/3} e^2(\rho_p^{4/3} + \rho_e^{4/3}) + f_e(\rho_e) + f_v(\rho_v) \right]. \quad (10)$$

The electrons are extremely relativistic and degenerate and are assumed to form a uniform negative background of density ρ_e . The neutrinos are also extremely degenerate and form also a uniform background of density ρ_v . They are decoupled from the other particles (except if we work at constant number of leptons per baryon. We shall come back to this point later) and their abundance is determined from beta equilibrium after the free energy reaches its minimum with respect to baryon and electron degrees of freedom. The expressions for f_e and f_v are standard and can be found in any astrophysics textbook (see for example Cox and Giuli, 1968).

At constant T , F/V has to be minimized for a given average baryon density

$$\rho_B = \frac{1}{V} \int d\bar{r} (\rho_n + \rho_p) \quad (11)$$

and average proton concentration Y_p

$$Y_p = \frac{1}{V\rho_B} \int d\bar{r} \rho_p(\bar{r}) \quad (12)$$

with the constraint of average charge neutrality

$$Y_e \equiv \frac{\rho_e}{\rho_B} = Y_p. \quad (13)$$

Under the conditions of interest here the nucleons can congregate into nuclei embedded in a lower density fluid or into bubbles in a higher density fluid. Both kinds of configurations will be referred to as nuclear clusters. Within the Wigner-Seitz (WS) approximation, we shall assume that each cluster, assumed spherically symmetric, occupies a cell of volume V_c and radius R_c in which the total electric charge is neutralized on the average. These cells are thus non interacting and the integration in equation (10) is restricted to only one of these cells.

To minimize equation (10) we have chosen a trial function approach with generalized Fermi functions for the densities

$$\rho_a = \frac{\rho_a^0}{\left[1 + \exp\left(\frac{r - R_q}{a_q}\right) \right]^{v_q}} + \rho_a^1. \quad (14)$$

The constant ρ_a^1 takes into account the non-vanishing nucleon density at the edge of the WS cell. δ_a is fixed to 1.5 for both kinds of nucleons. Due to equations (11) and (12), only three of the remaining density parameters are free. To reduce the number of variational parameters to two per density, the following relationship between the nuclear matter radius $r_0(Y_e, T)$, the particle number A and the parameter R_q and a_q was used ($\delta = 1.5$)

$$R_q = r_0 A^{1/3} \left[1 - \eta_v^{(0)} \frac{a_q}{r_0} A^{-1/3} + \frac{a_q^2}{r_0^2} A^{-2/3} (\eta_v^{(0)^2} - 2 \eta_v^{(1)}) + \frac{a_q^3}{r_0^3} A^{-1} \left(-\frac{2}{3} \eta_v^{(0)^3} + 2 \eta_v^{(0)} \eta_v^{(1)} - \eta_v^{(2)} \right) \right]. \quad (15)$$

The constants $\eta_v^{(u)}$ are defined by Krivine and Treiner (1981). An extra minimization with respect the WS radius R_c has to be performed to get the minimum of F/V . The pressure and chemical potentials of protons and neutrons were calculated by taking suitable numerical derivatives. Further technical details can be found in Barranco and Buchler (1981) and Marcos *et al.* (1982).

The trial function procedure has been criticized by some authors for its supposed lack of flexibility. It is worth emphasizing that it is not quite so. M. Brack *et al.* (1984) have shown that nuclear densities can be accurately described by functions only a bit more complicated than equation (14), provided a good prescription for the KED is used. One can see in Brack *et al.* (1984) how nicely the semiclassical densities agree with the HF ones at the surface, whereas inside the nucleus the former ones reproduce the average trend of the oscillating HF densities. At high temperature shell effects will disappear, improving even more that agreement.

What is obviously left out in our guess, equation (14), is the dip in the nuclear density near the center due to Coulomb repulsion among protons. But as shown by Brack *et al.* (1984), this is completely irrelevant as long as we are only interested in the total free energy. Moreover, the neutralizing electrons will decrease the effect of Coulomb repulsion.

⁽¹⁾ The explicit expressions of τ_{2q} and τ_{4q} are extremely cumbersome to write down explicitly. A printed output of nuclear subroutines and/or a computer tape with them is available from the authors on request.

We want to point out that the constraint (15) does not affect the final results in any appreciable amount while it reduces the computing time by at least a factor of two. Only the size of the high density bubbles changes noticeably and very likely the neutron chemical potential. The changes in size are however compatible with the big fluctuations in R_c present at high T and ρ_B .

So far, we have described the minimization procedure at constant T and Y_e . A few years ago, it was realized (Bethe *et al.*, 1979) that the collapse proceeds at almost constant entropy (S) and lepton concentration Y_1

$$Y_1 \equiv Y_e + \frac{\rho_\nu}{\rho_B}. \quad (16)$$

To keep S/A constant one has to iterate on T . Another readjustment of Y_e is needed in order to keep the total S (nucleon plus lepton) and Y_1 simultaneously constant. The procedure is straightforward but more time consuming. We shall present our results for fixed values of the nuclear plus electron entropy per baryon S/A and Y_e , as it is currently done in the literature. It turns out that the corresponding values of the total S/A and Y_1 are also almost constant.

4. Results.

Tables I to IX collect the EOS corresponding to the T6 interaction and constitute the main result of the present study. Let us discuss some of their features (for the explanation of the two lines marked with an asterisk in table II, see Sect. 5).

As we have stated before, a constant Y_e and S (nuclear plus electron) implies also an almost constant Y_1 and S_{tot} in this range of densities. The adiabatic index is close to $4/3$ when clusters are present.

The tables show that two different phase transitions (PT) take place. The first one from nuclei to bubbles and the second one from bubbles to homogeneous matter (HM). Observe that the number of nucleons clustered into bubbles is negative, meaning the nucleon default inside the cell. For HM, some entries in the tables have no meaning (as R_c for example) and were left out. Within our formalism, both PT are of first order. The PT from nuclei to bubbles was computed as suggested by Bonche and Vautherin (1982). The change in density was found to be very small (around 5% in most cases). It is worth noting that at both sides of that point, the regions where bubbles (nuclei) exist are rather wide : these regions are of metastability. As a matter of fact, it would be possible to consider the nucleus phase alone up to the point where the system becomes homogeneous (Hillebrandt *et al.*, 1984). In contradistinction, the transition from bubbles (nuclei) to HM is rather abrupt and we have not found any sizeable metastability region.

At low S and ρ_B , shell effects may play some role because the temperature is not very high (see tables I and II for example). However, the low density part of all the adiabats we present might be well described by nuclear statistical equilibrium (NSE) and shell effects will be automatically included in the calculation.

The plasma parameter Γ defined as

$$\Gamma = \frac{(Z_{cl} e)^2}{R_c T} \quad (17)$$

is an important quantity if one wants to estimate the contribution of plasma effects to the EOS. We shall come back to this point in section 5 but we anticipate that for $\Gamma > 170$ we deal with a Coulomb solid. We have found that the most general situation is the following (see table II for example). At low density we have a nucleus-like Coulomb liquid that becomes a Coulomb solid at higher densities. When the nucleus-to-bubble PT takes place, a bubble-like Coulomb solid is the most favoured configuration and finally near the bubble-to-HM PT, we have a Coulomb liquid made of bubbles.

The bubble-to-HM PT takes place at a rather low density even at low entropy. The stiffening of the EOS due to the nuclear incompressibility is quite apparent from the tables as we have already mentioned.

Figure 1 shows a typical EOS for $Y_e = 0.30$, $S/A = 1.5$ (all the figures were computed with T6). From low to high density, the three full line pieces correspond respectively to nuclei, bubbles and homogeneous NM. These pieces are disconnected because of the inability to study the coexistence of a system made of nuclei and bubbles simultaneously or bubbles and NM. One may see a part of metastable region (dashed line) corresponding to the nucleus-to-bubble PT. The dashed-dotted line is the EOS obtained within the so-called bulk-equilibrium approximation (Barranco and Buchler, 1980).

Another way to look at these PT is shown in figure 2. There we have plotted the enthalpy per particle W/A vs. pressure (Bonche and Vautherin, 1982). This figure shows again the three disconnected EOS pieces corresponding to nuclei (low p), bubbles (intermediate p) and NM (high p). The nucleus-to-bubble PT takes place very smoothly. Indeed, one can see that the metastable nucleus and bubble phases, represented by dashed lines, are very nearly equal to the stable phase on both sides of the transition point.

The NM part of the EOS was calculated as indicated by Barranco and Buchler (1980; 1981). This part of the EOS is extremely easy and fast to compute with complete, well behaved Skyrme-like forces. Consequently, up to the density where one can trust the approach based on the existence of a mean field potential and mesonic degrees of freedom do not play any appreciable role, we see no advantage in introducing *ad hoc* parametrizations of the EOS as a function of K , the adiabatic index and any other nuclear property as saturation density, binding energy or symmetry energy (Baron *et al.*, 1984). We have stopped our calculations at $\rho_B = 0.30 \text{ fm}^{-3}$ but we are aware of the limitations of the approach at such high densities.

Another point to be stressed is the important thermal fluctuations that make the nucleon content of the cell rather uncertain. They are shown for the cases $S/A = 1$; $Y_e = 0.35$ and 0.30 for SkM force and $S/A = 1.5$, $Y_e = 0.35$ for T6 (tables X, XI and VII respectively). These fluctuations are typically $\delta A/A \sim 15\text{-}30\%$ and increase at higher density and/or entropy.

Tables X and XI were computed with the force SkM and table XII with the force S1' of Lamb *et al.* (1978).

Table X allows for a direct comparison of the present method with the THF results of Bonche and Vautherin (1982) and the variational TTF calculations of Suraud (1984) (note that they used $Y_e = 0.285$). One can see that the agreement is reasonable apart from a not unexpected difference in μ_n and A/Z .

The forces T6 and SkM yield very similar adiabatic indexes whereas S1' gives much bigger values of γ . Observe that the pressures are very similar for the three forces up to the point where bubbles merge. Note also the different values of T due to the different m^* .

Figure 3 shows the isentrops $\log T$ vs. $\log \rho_B$ for $Y_e = 0.35$. This figure corresponds to figure 3 of Hillebrandt *et al.* (1984) where a marked discontinuity is shown for $S/A = 1$. It has been argued by Lattimer *et al.* (1985) that such pathology could be due to the fact that they did not consider the possible existence of bubbles in their calculation. They used Kohler's Ska force (Kohler, 1976) which has $K = 263$ MeV, $m^*/m = 0.61$ and a symmetry energy of 32.9 MeV, the rest of its properties being rather standard.

We may assert that it is not due to the lack of bubble configurations. Indeed, we have computed the adiabats $S/A = 1$, $Y_e = 0.30$ and 0.35 with T6 and found that at $\rho_B = 0.10 \text{ fm}^{-3}$ the difference in T between nucleus and bubble configurations was around two per cent. The same difference was found for the total pressure. The comparison of tables II and X shows that it cannot be an effective mass effect either (although $m^*/m = 0.6$ is too small).

To end up with this section we would like to comment on the influence of the gradient corrections to the kinetic energy and to the entropy. Table XIII shows the results corresponding to T6, $S/A = 1$, $Y_e = 0.30$ for densities $\rho_B = 0.04$ and 0.08 fm^{-3} . The first line is the result already shown in table II. The second line was obtained improving the present approach by correcting up to second order in \hbar (i.e. including a gradient correction) the expression of the entropy (Brack, 1984). The third line is the zeroth order TF result computed following Marcos *et al.* (1982). One may see that lines one and two agree reasonably well but in general the results obtained with the crudest TF model (third line) are very close to the most sophisticated one (second line). Other tests performed at different densities and entropies yielded similar results.

We want to point out that we were aware of Brack's correction when a big part of our calculation was done so we decided not to include that small correction and just checked its influence on the results. Actually, there is no difficulty in taking into account any gradient term in $s(\rho, \tau)$.

5. Plasma effects.

Among the effects left out in the formalism so far presented one might include the so-called plasma effects. These effects arise because, due to thermal motion, the nuclear cluster as a whole has a translational or vibrational energy and an extra Coulomb energy (« Coulomb excess »).

Both extra energies are well known by plasma physicists and explicit expressions have been worked out for the one component plasma (OCP) (Hansen, 1973; Pollock and Hansen, 1973; Slattery *et al.*, 1980). The application of these

results to the EOS problem has to be done with some caution. Indeed, they were obtained from an opposite point of view to the one we have adopted for EOS calculations, i.e. one particle (cluster) in one WS cell. In OCP calculations one tries to follow the evolution of as many particles as possible inside a given volume. Moreover, OCP calculations always treat the particles as point-like, structureless entities. This is far from one finite nucleus whose radius is sometimes around half the radius of its WS cell. Although some prescriptions may be adopted to correct the limitations of the OCP results (Lattimer *et al.*, 1985) they are far from being well established from the plasma physics point of view.

It is however interesting to use the OCP expressions to have an estimate of these effects, at least qualitatively. Here we closely follow the method proposed by Barranco and Buchler (1981).

Presently, it is well established that the OCP constitutes a Coulomb liquid for $\Gamma < 170$, whereas for $\Gamma > 170$ we have to deal with a Coulomb solid. Since at high T and ρ_B the system is in the strong coupling limit ($\Gamma \gg 1$), we use for the Coulomb excess free energy the expressions obtained by Slattery *et al.* (1980). It is easy to verify that the plasma free energy (translational plus Coulomb excess) reads

$$\frac{F_{\text{pl}}^L}{T} = -0.89752 \Gamma + 3.78176 \Gamma^{1/4} - 0.71816 \Gamma^{-1/4} + 2.19951 \ln \Gamma + 2.23221 + \frac{3}{2} \ln \frac{T}{A_{\text{cl}}(Z_{\text{cl}})^4} \quad (18)$$

for the liquid phase (i.e. $\Gamma < 170$) and

$$\frac{F_{\text{pl}}^S}{T} = -0.89752 \Gamma - \frac{1490}{\Gamma^2} + \frac{9}{2} \ln \Gamma + 3.6477 + \frac{3}{2} \ln \frac{T}{A_{\text{cl}}(Z_{\text{cl}})^4} \quad (19)$$

for the solid phase. A few comments are now in order. First of all, the first term $\sim -9/10 \Gamma$ is already included in the proton-electron Coulomb energy, so it has to be dropped out from these expressions. Second, F_{pl} is the *total* free energy per WS cell (in MeV) that has to be added to the previous results if one wants to correct them for plasma effects (remember T is in MeV). $A_{\text{cl}}(Z_{\text{cl}})$ are the number of clustered nucleons (protons) and no correction of volume excluded type has been made in the translational (vibrational) free energy. Indeed, if one writes the translational free energy

$$\frac{F_{\text{tr}}}{T} = \ln \left[\frac{1}{V_c} \left(\frac{2 \pi \hbar^2}{m A_{\text{cl}} T} \right)^{3/2} \right] - 1 \quad (20)$$

and wants to correct V_c for the volume occupied by the nucleus V_n , it is obvious from the tables that in the region where the system constitutes a Coulomb liquid, V_n is negligible in front of V_c . Indeed, if $V_n = 4/3 \pi r_0^3 / A$ with $r_0 = 1.2 \text{ fm}$ one has :

$$\frac{V_n}{V_c} \approx \left[\frac{r_0 A^{1/3}}{R_c} \right]^3 \ll 1. \quad (21)$$

Moreover, for a diffuse nucleus it is quite arbitrary to associate a certain volume to it.

What worsens the situation is the large uncertainty in the values of A and Z due to thermal fluctuations. Consequently, we do not consider of any relevance to improve on these equations, given the intrinsic uncertainties in its primordial ingredients (V_c , A_{c1} , Z_{c1}). It is also obvious from the tables that at high density, the system is a Coulomb solid, so special attention should be paid to equation (19) rather than to equation (18).

An additional difficulty arises when bubbles take over since it is not clear what the « mass » of a bubble is. We have assumed that A_{c1} and Z_{c1} the mass and charge default inside the cell and checked that the nucleus-to-bubble (NB) phase transition is still smooth.

We have estimated the plasma effects perturbatively and also included them explicitly in the minimization. In the few cases we have computed, there is no appreciable difference between both methods. We have also verified that the NB phase transition is not much affected either, although because of the uncertainties already mentioned, F_{p1} should not be considered when determining the NB transition.

The contribution of these effects to the *total* pressure and *total* entropy (not per baryon) can be obtained from :

$$P_{p1} = \frac{\Gamma}{4\pi R_c^3} \frac{\partial F_{p1}}{\partial \Gamma} \quad (22)$$

$$S_{p1} = -\frac{F_{p1}}{T} - \frac{3}{2}. \quad (23)$$

As a detailed example of the influence of plasma effects in the variational calculation, we have included in table II two lines marked with an asterisk for $\rho_B = 0.01$ and 0.04 fm^{-3} which were computed including in the minimization equations (18) and (19) respectively. Plasma effects tend to decrease the cluster size without changing appreciably the other quantities.

Finally, table XIV shows the contribution of these effects to F/A , P and S/A computed perturbatively (Eqs. (18)-(19) and (22)-(23)) along the $S/A = 1$, $Y_e = 0.30$ adiabat, always for the T6 force.

6. Alpha particles.

Trying to go a step beyond the pure WS approximation, some authors have included in the calculation alpha particles either within the so-called bulk approximation (i.e., neglecting Coulomb and finite size effects) (Barranco and Buchler, 1981; Pi *et al.*, 1983) or within the WS approximation (Lamb *et al.*, 1978; Lattimer *et al.*, 1985).

Since alpha particles plus bulk matter have been studied with some detail in the first two references above, let us say a few words about the possibility of including alphas in the full WS formalism. The cleanest way of including them would be to consider a nuclear WS cell surrounded by satellite alpha particle WS cells. In this way, one would not need to pay any attention to Coulomb interaction between alphas and the nuclear cluster although some problems might arise because very likely, different electron

densities would be needed inside the nuclear WS and the alpha WS cells. Unfortunately, this procedure has to be ruled out because the small charge of the alpha particle and the high temperatures involved make the plasma parameter Γ much smaller than one :

$$1 \gg \frac{(Z_\alpha e)^2}{R_\alpha T}. \quad (24)$$

This is the Debye-Hückel limit (Landau and Lifshitz, 1967) and definitely the WS approximation has no sense under these conditions.

It would be also possible to allow the alpha particles to float around inside the nuclear WS cell (Lamb *et al.*, 1978; Lattimer *et al.*, 1985). In this case, the procedure is much less transparent because of all the complexities associated with binary Coulomb mixtures (see for example Brama *et al.*, 1979). A brute force calculation might consist in minimizing the quantity

$$\frac{F}{V} = \frac{1}{V_c} F_N + n_\alpha f_\alpha \quad (25)$$

where F_N/V_c is the whole expression (10), n_α is the number of alphas per unit volume and f_α the free energy per alpha, without paying any attention to plasma effects and obviously imposing charge and baryon conservation inside the WS cell.

We do believe that this method is extremely fraught with danger because we cannot control the approximations we make. If many nuclear species are expected to be in NSE at low ρ_B and/or T it would be better to use NSE up to that point and then switch to the WS, one nucleus approximation, matching both pieces of EOS. Indeed, Hillebrandt *et al.* (1984) have shown that it can be done smoothly. For these reasons, we have left out alpha particles in our calculation. Moreover, they are very rare in the region of the $\rho_B - T$ plane in which we are interested (Pi *et al.*, 1983).

7. Conclusions.

We have presented a detailed EOS computed with a reliable nuclear force and using one of the best semiclassical formalisms available. Comparisons have been made with other methods and between the EOS obtained with different forces. These forces yield similar EOS although there are obvious differences between forces having extreme different nucleon effective masses or nuclear incompressibilities.

The agreement with THF calculations is in general satisfactory, the remaining differences being due to our very restricted trial densities. Had we used the four parameter density (Eq. (14)) without any restriction, the agreement would have been even more satisfactory. However, our goal of an extense tabulation has prevented us from using more flexible densities.

The present spherical WS approach constitutes a compromise between reliability and computing time. As we have stated at the introduction, nonspherical clusters come into play at densities around half the NM

saturation density value. These exotic forms are interesting from a pure theoretical point of view, but we are far from having an extense EOS tabulation that will include them.

Corrections to the one nucleus WS approach have been worked out (Lamb *et al.*, 1984 : Burrows and Lattimer, 1984) and found to be small. Plasma effects have also been estimated, but not included all over the calculation. It seems to us of little justification to include some effects in the calculation and to leave out others of similar importance.

References

- BARON, E., COOPERSTEIN, J., KAHANA, S. : 1985, *Nucl. Phys.* in press.
 BARRANCO, M., BUCHLER, J. R. : 1980, *Phys. Rev. C* **22**, 1729.
 BARRANCO, M., BUCHLER, J. R. : 1981, *Phys. Rev. C* **24**, 1191.
 BARRANCO, M., TREINER, J. : 1981, *Nucl. Phys. A* **351**, 269.
 BARRANCO, M., PEREZ-CANYELLAS, A., PI, M., POLLS, A., VINAS, X. : 1984, contributed paper, 8th Workshop on Condensated Matter Theories. Granada, Spain. An. Fis. (Spain), in press.
 BARTEL, J., QUENTIN, Ph., BRACK, M., GUET, C. and HAKANSSON, H. B. : 1982, *Nucl. Phys. A* **386**, 79.
 BEINER, M., FLOCARD, H., GIAI, N. V., QUENTIN, Ph. : 1975, *Nucl. Phys. A* **238**, 29.
 BETHE, H. A., BROWN, G. E., APPLGATE, J., LATTIMER, J. M. : 1979, *Nucl. Phys. A* **324**, 487.
 BOHIGAS, O., CAMPI, X., KRIVINE, H., TREINER, J. : 1976, *Phys. Lett. B* **64**, 381.
 BOHIGAS, O., LANE, A. M., MARTORELL, J. : 1979, *Phys. Rep. C* **51**, 267.
 BONCHE, P., VAUTHERIN, D. : 1981, *Nucl. Phys. A* **372**, 496.
 BONCHE, P., VAUTHERIN, D. : 1982, *Astron. Astrophys.* **112**, 268.
 BRACK, M. : 1983, NATO ASI Summer School on Density Functional Methods in Physics, Alcabideche, Portugal 5-16 September.
 BRACK, M. : 1984, *Phys. Rev. Lett.* **53**, 119.
 BRACK, M., GUET, C., HAKANSSON, H. B. : 1985, *Phys. Rep.* **123**, 275.
 BRAMI, B., HANSEN, J. P. and JOLY, F. : 1979, *Physica A* **95**, 505.
 BROWN, G. E., GUNN, J. H., GOULD, P. : 1963, *Nucl. Phys.* **46**, 598.
 BURROWS, A., LATTIMER, J. M. : 1984, Stony Brook preprint.
 COTE, J., PEARSON, J. M. : 1978, *Nucl. Phys. A* **304**, 104.
 COX, J. P., GIULI, R. T. : 1968, *Principles of Stellar Structure* (Gordon and Breach, New York).
 EL EID, M. F., HILLEBRANDT, W. : 1980, *Astron. Astrophys. Suppl. Ser.* **42**, 215.
 FRIEDMAN, B., PANDHARIPANDE, V. R. : 1981, *Nucl. Phys. A* **361**, 502.
 GRAMMATICOS, B., VOROS, A. : 1980, *Ann. Phys.* **129**, 153.
 HANSEN, J. P. : 1973, *Phys. Rev. A* **8**, 3096.
 HARTMANN, D., EL EID, M. F., BARRANCO, M. : 1984, *Astron. Astrophys.* **131**, 249.
 HASHIMOTO, M., HIRONORI, S., YAMADA, M. : 1984, *Prog. Theor. Phys.* **71**, 320.
 HILLEBRANDT, W., NOMOTO, K., WOLFF, R. G. : 1984, *Astron. Astrophys.* **133**, 175.
 JEUKENNE, J. P., LEJEUNNE, A., MAHAUX, C. : 1976, *Phys. Rep. C* **25**, 83.
 KOHLER, S. : 1976, *Nucl. Phys. A* **258**, 301.
 KRIVINE, H., TREINER, J., BOHIGAS, O. : 1980, *Nucl. Phys. A* **351**, 269.
 KRIVINE, H., TREINER, J. : 1981, *J. Math. Phys.* **22**, 2484.
 LAMB, D. Q., LATTIMER, J. M., PETHICK, C. J., RAVENHALL, D. G. : 1978, *Phys. Rev. Lett.* **41**, 1623.
 LANDAU, L., LIFSHITZ, E. : 1967, *Physique Statistique* (Editions Mir, Moscow).
 LATTIMER, J. M., PETHICK, C. J., RAVENHALL, D. G., LAMB, D. Q. : 1985, *Nucl. Phys. A* **432**, 646.
 LOMBARD, R. J. : 1973, *Ann. Phys.* **77**, 380.
 MARCOS, S., BARRANCO, M., BUCHLER, J. R. : 1982, *Nucl. Phys. A* **381**, 507.
 MAZUREK, T. J., LATTIMER, J. M., BROWN, G. E. : 1979, *Astrophys. J.* **229**, 713.
 NEGELE, J. W., VAUTHERIN, D. : 1975, *Phys. Rev. C* **11**, 1031.
 OGASAWARA, R., SATO, K. : 1983, *Prog. Theor. Phys.* **70**, 1569.
 OGASAWARA, R. : 1985, *Prog. Theor. Phys.* **73**, 367.
 OYAMATSU, K., HASHIMOTO, M., YAMADA, M. : 1984, *Prog. Theor. Phys.* **72**, 373.
 PI, M., BARRANCO, M., MARCOS, S. : 1983, *Il Nuovo Cim. A* **75**, 100.
 POLLOCK, E. L., HANSEN, J. P. : 1973, *Phys. Rev. A* **8**, 3110.
 RAVENHALL, D. G., PETHICK, C. J., WILSON, J. R. : 1983, *Phys. Rev. Lett.* **50**, 2066.
 RAYET, M., ARNOULD, M., TONDEUR, F., PAULUS, G. : 1982, *Astron. Astrophys.* **116**, 183.
 SIEMENS, P. J. : 1984, *Nucl. Phys. A* **428**, 189c.
 SLATTERY, W. L., DOOLEN, G. D., DE WITT, H. E. : 1980, *Phys. Rev. A* **21**, 2087.
 SURAUD, E. : 1984, These de 3^e cycle Orsay (unpublished).
 SURAUD, E., VAUTHERIN, D. : 1984, *Phys. Lett. B* **138**, 325.
 TONDEUR, F., BRACK, M., FARINE, M., PEARSON, J. M. : 1984, *Nucl. Phys. A* **420**, 297.
 VIÑAS, X., BARRANCO, M., PI, M., POLLS, A., PEREZ-CANYELLAS, A. : 1984, *J. Physique Colloq.* **45**, C6-103.
 VIÑAS, X., GARCIA-ROGER, J., BARRANCO, M. : 1981, *Phys. Lett. B* **100**, 209.
 WILLIAMS, R. D., KOONIN, S. E. : 1985, *Nucl. Phys. A* **435**, 844.
 WOLFF, R. : 1983, Proceedings of the Ringberg Castle Workshop on Nuclear Astrophysics, Tegernsee, FRG 6-10 June.

Acknowledgements.

We are most indebted to François Tondeur for useful correspondence. We want to thank Matthias Brack for his guidance through the ETF method and Dieter Hartmann and Joan Martorell for several interesting discussions. One of us (A. Perez) wishes to thank the Centro de Calculo of the Universidad Politecnica de Valencia for its collaboration. This work has been supported in part by the CAICYT (Spain) (Grant 1348/82) and by a grant of the University of Barcelona.

TABLE I. — EOS for T6 along the S/A = 0.70, Y_e = 0.50.

T	R _c	A/Z	A _{e1} /Z _{e1}	Γ	P _{***}	μ _n	μ _p	μ _B	P _{tot}	F _{tot} /A	S _{tot} /A	Y _e	
(fm ⁻³)	(MeV)	(fm)			(MeVfm ⁻³)	(MeV)	(MeV)	(MeV)	(MeVfm ⁻³)	(MeV)	(MeV)		
.001	1.02	32.14	139/42	124/42	77	-0.030	-1.47	-22.91	40.8	.0031	1.50	.707	.313
.005	1.75	20.50	180/54	163/54	119	-0.255	-1.36	-25.52	49.7	.0277	8.49	.715	.339
.01	2.13	17.4	221/66	201/66	170	.0637	-1.21	-27.52	87.9	.0711	13.08	.717	.349
.02	2.62	15.34	303/91	280/91	295	.1998	-1.00	-30.28	110.7	.1819	18.92	.719	.357
.03	2.93	14.70	399/120	373/120	478	.2704	-0.86	-32.36	126.7	.3140	23.02	.719	.361
.04	3.16	14.57	519/156	487/156	756	.3939	-0.78	-35.02	139.5	.4618	26.29	.719	.364
.05	3.35	14.79	671/203	638/203	1197	.5248	-0.72	-37.52	150.3	.6218	29.03	.719	.366
.06	3.51	15.25	891/267	840/267	1913	.6674	-0.68	-39.87	159.7	.7921	31.42	.720	.368
.07	3.64	16.13	1231/369	1104/411	4138	.7700	-1.39	-38.66	168.2	.9264	33.45	.719	.369
.08	3.76	14.72	1070/321	858/269	1881	.9223	-1.30	-40.24	175.8	1.1108	35.23	.719	.369
.09	3.88	13.51	929/279	557/174	832	1.0766	-1.24	-41.31	182.9	1.3017	36.87	.719	.369
.10	3.98	12.35	789/237	344/108	339	1.2398	-1.23	-42.71	189.4	1.4974	38.40	.719	.370
.11	3.90					1.251	-2.78	-43.94	195.5	1.556	40.44	.718	.372
.12	4.12					1.524	-1.72	-44.71	201.3	1.862	41.45	.718	.371
.13	4.34					1.840	-0.49	-45.10	206.7	2.212	42.51	.719	.371
.14	4.55					2.202	.94	-45.12	211.9	2.611	43.62	.719	.370
.15	4.75					2.615	2.55	-44.80	216.8	3.061	44.78	.719	.370
.18	5.33					4.181	8.44	-41.19	230.3	4.751	46.61	.720	.370
.20	6.05					5.927	13.20	-35.85	246.2	6.192	51.48	.722	.372
.22	6.56					7.141	16.37	-33.42	256.9	7.910	54.59	.722	.372
.28	7.04					10.11	27.71	-25.04	256.9	11.06	59.76	.724	.374
.30	7.36					13.78	38.09	-14.06	266.7	14.94	65.52	.725	.377
						16.65	45.65	-5.60	272.9	17.98	69.49	.726	.379

TABLES I TO XII. — ρ_B is the baryon density, T the temperature, R_c the WS cell radius, A/Z the number of baryons/protons inside the cell, A_{e1}/Z_{e1} the number of clustered baryons (negative values of A_{e1} and Z_{e1} correspond to bubble configurations), Γ is the plasma parameter, P_{N+e} the nuclear plus electron pressure, μ_n , μ_p and μ_B the neutron, proton and electron chemical potentials (μ_n can be obtained from $\mu_p = \mu_n - \mu_n + \mu_e - 1.3$ MeV). The entries with the subscript tot include the neutrino contribution. S/A is always in units of Boltzmann's constant ks. Y_e is the lepton fraction per baryon and γ is the adiabatic index. Some of these γ are average values computed in a range of ρ_B corresponding to either nuclei or bubbles.

TABLE II. — The same as table I for S/A = 1 (see section 5 for the explanation of the two lines marked with an asterisk).

T	R _c	A/Z	A _{e1} /Z _{e1}	Γ	P _{***}	μ _n	μ _p	μ _B	P _{tot}	F _{tot} /A	S _{tot} /A	Y _e	
(fm ⁻³)	(MeV)	(fm)			(MeVfm ⁻³)	(MeV)	(MeV)	(MeV)	(MeVfm ⁻³)	(MeV)	(MeV)		
.001	1.51	30.66	121/36	104/36	41	.0030	-2.71	-21.19	40.7	.0031	1.25	1.018	.321
.005	2.49	20.16	172/52	148/51	76	.0265	-2.54	-24.12	69.6	.0293	6.16	1.024	.344
.01	3.09	17.03	207/62	181/62	105	.0681	-2.38	-26.49	87.7	.0748	12.60	1.028	.354
.02	3.78	14.93	278/84	248/83	177	.1641	-2.20	-28.73	87.7	.0750	12.85	1.028	.353 (†)
.03	4.23	14.25	364/109	329/109	283	.2788	-2.03	-32.16	126.5	.3254	22.14	1.029	.364
.04	4.56	14.12	471/141	429/141	444	.4053	-1.93	-34.13	139.3	.4768	25.27	1.028	.366
.05	4.80	13.57	419/126	381/126	372	.4080	-1.86	-34.08	139.3	.4792	25.28	1.028	.366 (†)
.06	4.84	14.33	617/185	565/184	706	.5419	-1.86	-35.87	150.0	.6404	27.89	1.028	.368
.07	5.07	15.09	1008/302	953/300	1634	.6853	-1.83	-37.42	159.4	.8135	32.05	1.029	.369
.08	5.43	13.76	872/262	612/192	713	.9421	-2.42	-41.28	175.5	1.3294	33.80	1.027	.369
.09	5.59	12.58	750/225	382/120	295	1.1046	-2.37	-42.61	182.6	1.3287	35.38	1.027	.370
.10	5.73	11.17	584/175	205/65	96	1.2677	-2.39	-43.85	189.1	1.5273	36.86	1.027	.370
.11	5.74					1.352	-3.19	-44.80	195.2	1.656	38.75	1.028	.372
.12	6.07					1.640	-2.18	-45.61	201.0	1.977	39.67	1.027	.371
.13	6.38					1.972	-0.97	-46.04	206.4	2.343	40.64	1.027	.370
.14	6.69					2.351	.44	-46.11	211.5	2.758	41.66	1.028	.370
.15	6.99					2.781	2.03	-45.83	216.4	3.226	42.74	1.028	.370
.18	7.84					4.405	7.86	-43.02	229.8	4.973	46.32	1.030	.370
.20	8.38					5.793	12.58	-39.63	238.0	6.445	49.03	1.031	.370
.22	8.89					7.450	17.81	-35.13	245.6	8.218	52.00	1.032	.371
.25	9.63					10.49	27.01	-26.43	256.2	11.43	56.94	1.034	.374
.28	10.34					14.24	37.34	-15.53	266.0	15.40	62.48	1.036	.376
.30	10.80					17.16	44.87	-7.13	272.1	18.48	66.51	1.038	.379

TABLE III. — The same as table I for S/A = 1.5.

T	R _c	A/Z	A _{e1} /Z _{e1}	Γ	P _{***}	μ _n	μ _p	μ _B	P _{tot}	F _{tot} /A	S _{tot} /A	Y _e	
(fm ⁻³)	(MeV)	(fm)			(MeVfm ⁻³)	(MeV)	(MeV)	(MeV)	(MeVfm ⁻³)	(MeV)	(MeV)		
.001	2.29	31.22	127/38	101/38	29	.0034	-4.71	-18.30	40.4	.0037	.65	1.535	.340
.005	3.75	19.50	155/47	124/46	42	.0290	-4.77	-22.15	69.2	.0329	7.22	1.543	.360
.01	4.62	16.30	181/54	147/53	54	.0718	-4.66	-25.19	87.2	.0829	11.28	1.544	.365
.02	5.69	14.09	234/70	194/69	85	.1775	-4.51	-29.47	110.0	.2069	16.29	1.543	.367
.03	6.37	13.35	299/90	232/88	130	.3001	-4.40	-32.61	125.9	.3517	19.79	1.544	.369
.04	6.90	13.20	386/116	327/112	200	.4332	-4.35	-35.12	138.6	.5119	22.59	1.543	.369
.05	7.35	13.39	503/151	429/147	316	.5805	-4.36	-37.31	149.4	.6848	24.90	1.544	.370
.06	7.72	13.89	674/202	573/195	512	.7339	-4.35	-39.28	159.7	.8675	26.91	1.542	.370
.07	7.94	13.14	665/199	499/150	311	.8675	-5.01	-42.04	167.2	1.0004	28.72	1.541	.370
.08	8.24	11.55	516/155	242/79	94	1.0652	-5.04	-43.68	174.8	1.2003	30.24	1.542	.370
.09	8.17					1.081	-5.84	-44.39	181.9	1.320	32.79	1.540	.372
.10	8.73					1.326	-5.34	-46.19	185.3	1.915	33.35	1.541	.371
.11	9.27					1.610	-4.61	-47.56	194.3	1.910	33.96	1.542	.370
.12	9.30					1.937	-3.67	-48.52	200.3	2.270	34.62	1.543	.369
.13	10.30					2.311	-2.53	-49.09	205.3	2.677	35.34	1.543	.369
.14	10.78					2.733	-1.19	-49.28	210.4	3.135	36.11	1.544	.368
.15	11.26					3.208	.33	-49.13	215.2	3.647	36.95	1.545	.368
.18	12.62					4.977	5.98	-46.68	228.5	5.339	39.85	1.547	.368
.20	13.49					6.470	10.59	-43.52	236.5	7.126	42.12	1.549	.369
.22	14.29					8.240	15.81	-39.23	244.0	9.000	44.67	1.551	.370
.25	15.47					11.46	24.76	-30.83	254.4	12.39	49.00	1.554	.372
.28	16.59					15.40	34.94	-20.22	263.9	16.55	53.95	1.557	.375
.30	17.31					18.46	42.38	-12.00	270.0	19.77	57.99	1.559	.377

TABLE V. — The same as table I for S/A = 0.7 and Y_e = 0.35.

Table with 13 columns: T, R_c, A/Z, A_cst/Z_cst, Gamma, P_nuc, mu_n, mu_p, mu_e, P_nuc, F_nuc/A, S_nuc/A, Y_i, Y_e. Rows range from 0.001 to 0.30.

TABLE VII. — The same as table V for S/A = 1.5.

Table with 13 columns: T, R_c, A/Z, A_cst/Z_cst, Gamma, P_nuc, mu_n, mu_p, mu_e, P_nuc, F_nuc/A, S_nuc/A, Y_i, Y_e. Rows range from 0.001 to 0.30.

TABLE IV. — The same as table I for S/A = 2.

Table with 13 columns: T, R_c, A/Z, A_cst/Z_cst, Gamma, P_nuc, mu_n, mu_p, mu_e, P_nuc, F_nuc/A, S_nuc/A, Y_i, Y_e. Rows range from 0.001 to 0.30.

TABLE VI. — The same as table V for S/A = 1.

Table with 13 columns: T, R_c, A/Z, A_cst/Z_cst, Gamma, P_nuc, mu_n, mu_p, mu_e, P_nuc, F_nuc/A, S_nuc/A, Y_i, Y_e. Rows range from 0.001 to 0.30.

TABLE IX. — The same as table I for $S/A = I$ and $Y_e = 0.40$.

T	R_c	M/Z	β_{c1}/Zc_1	Γ	P_{max}	μ_n	μ_p	μ_e	P_{eet}	F_{eet}/A	S_{eet}/A	Y_e	
(m^{-2}) (MeV)	(fm)				(MeV m^{-3})	(MeV)	(MeV)	(MeV)	(MeV m^{-3})	(MeV)	(MeV)		
.001	2.26	27.96	97/37	86/36	30	-0.045	-7.44	-14.11	44.6	-0.056	6.23	1.070	.514
.005	3.15	17.62	119/47	113/47	57	-0.075	-7.86	-16.75	76.5	-0.086	18.15	1.061	.531
.01	3.61	15.15	146/58	140/58	88	-0.0935	-8.01	-18.50	96.5	-0.127	25.60	1.057	.536
.02	4.13	13.41	202/81	196/80	167	-0.239	-8.23	-20.79	121.6	-0.392	34.97	1.053	.540
.03	4.46	12.89	249/107	243/107	287	-0.398	-8.45	-22.41	139.3	-0.5302	41.57	1.049	.542
.04	4.71	12.84	335/142	327/141	473	-0.576	-8.64	-23.77	153.3	-0.7762	46.78	1.049	.543
.05	4.92	13.07	460/187	450/186	777	-0.7745	-8.84	-24.96	165.2	-1.0424	51.15	1.047	.544
.06	5.11	13.53	622/249	612/248	1278	-0.9819	-9.03	-26.07	175.6	-1.3249	54.94	1.047	.544
.07	5.22	14.18	837/335	827/330	2816	-1.1406	-10.17	-29.16	193.3	-1.6684	58.23	1.045	.544
.08	5.37	12.97	731/292	720/282	1317	-1.3466	-10.43	-31.24	208.3	-2.0685	66.10	1.042	.543
.09	5.51	11.92	638/255	628/250	606	-1.6001	-10.28	-30.21	201.1	-2.1857	63.67	1.044	.543
.10	5.62	10.81	527/211	517/201	243	-1.8564	-10.45	-31.24	205.0	-2.5085	66.10	1.042	.543
.11	5.81	10.81	527/211	517/201	243	-1.8564	-10.45	-31.24	205.0	-2.5085	66.10	1.042	.543
.12	5.82	11.42	622/249	612/248	1278	-2.276	-11.22	-32.78	221.3	-3.1628	71.00	1.042	.544
.13	6.12	12.97	731/292	720/282	1317	-2.712	-11.24	-32.62	227.3	-3.6739	72.79	1.042	.544
.14	6.41	14.18	837/335	827/330	2816	-3.182	-9.03	-32.13	233.0	-4.2409	74.60	1.043	.544
.15	6.69	15.15	1046/77	1036/76	4733	-3.708	-7.98	-31.34	238.4	-4.8675	76.44	1.044	.544
.16	7.00	17.62	146/58	140/58	88	-4.356	-1.96	-27.20	253.2	-7.1378	82.17	1.047	.544
.18	7.50	15.15	146/58	140/58	88	-5.856	-2.81	-23.09	262.2	-9.0082	86.21	1.048	.544
.20	8.01	13.41	202/81	196/80	167	-7.283	8.32	-17.98	270.6	-11.921	90.47	1.050	.545
.22	8.50	12.89	249/107	243/107	287	-9.228	17.92	-8.55	282.3	-15.1049	97.28	1.052	.547
.25	9.20	12.84	335/142	327/141	473	-12.74	29.01	2.84	293.1	-19.8956	104.57	1.054	.549
.28	9.87	13.07	460/187	450/186	777	-17.03	37.18	11.46	299.9	-23.4998	109.74	1.056	.551
.30	10.30	13.53	622/249	612/248	1278	-20.37							

TABLE XI. — The same as table X for $Y_e = 0.35$.

T	R_c	M/Z	β_{c1}/Zc_1	Γ	P_{max}	μ_n	μ_p	μ_e	P_{eet}	F_{eet}/A	S_{eet}/A	Y_e		
(m^{-2}) (MeV)	(fm)				(MeV m^{-3})	(MeV)	(MeV)	(MeV)	(MeV m^{-3})	(MeV)	(MeV)			
.001	1.99	28.99	102/36	92/36	32	-0.038	-5.24	-17.36	42.7	-0.043	2.91	1.038	.408	.14
.005	2.99	18.38	130/46	119/45	54	-0.020	-3.38	-19.99	73.2	-0.083	12.31	1.045	.435	.17
.01	3.57	15.56	158/55	145/55	78	-0.079	-5.41	-21.91	92.2	-0.075	18.24	1.044	.443	.18
.02	4.24	13.70	215/75	200/75	139	-0.190	-5.42	-24.54	116.3	-0.271	25.68	1.043	.449	.18
.03	4.68	13.14	285/100	267/99	230	-0.338	-5.46	-26.47	133.1	-0.424	30.88	1.045	.451	.18
.04	5.01	13.10	374/132	355/131	377	-0.4935	-5.51	-28.06	146.6	-0.622	35.01	1.041	.453	.17
.05	5.28	13.32	495/173	468/172	608	-0.6593	-5.59	-29.47	157.9	-0.852	38.47	1.041	.454	.17
.06	5.48	13.50	618/216	588/215	903	-0.8316	-5.68	-30.81	167.8	-1.0578	41.49	1.039	.455	.17
.07	5.69	14.40	812/319	848/311	1621	-0.9759	-6.45	-33.06	176.6	-1.2532	43.77	1.041	.455	.17
.08	6.09	15.20	770/270	720/270	1151	-1.1712	-6.41	-34.35	184.7	-1.5019	45.98	1.040	.455	.17
.09	6.28	12.02	652/229	633/213	250	-1.3755	-6.39	-35.55	192.1	-1.7600	48.02	1.040	.455	.17
.10	6.47	10.82	537/186	518/187	62	-1.5797	-6.43	-36.71	199.0	-2.0240	49.90	1.040	.455	.17
.11	6.47	10.82	537/186	518/187	62	-1.5797	-6.43	-36.71	199.0	-2.0240	49.90	1.040	.455	.17
.12	6.91	12.97	731/292	720/282	1317	-1.982	-6.81	-36.83	205.4	-2.286	52.43	1.039	.457	.18
.13	7.35	15.15	1046/77	1036/76	4733	-2.120	-5.71	-37.36	211.4	-2.695	55.63	1.040	.456	.18
.14	7.78	17.62	146/58	140/58	88	-2.921	-4.39	-37.57	217.1	-3.152	58.85	1.041	.455	.18
.15	8.21	15.15	146/58	140/58	88	-2.973	-2.86	-37.47	222.5	-3.661	58.09	1.042	.454	.18
.18	9.49	13.41	202/81	196/80	167	-3.478	5.21	-34.29	241.7	-6.281	61.40	1.047	.451	.238
.20	10.34	12.89	249/107	243/107	287	-4.913	10.32	-31.17	250.2	-7.979	64.29	1.049	.450	.2304
.22	11.18	12.84	335/142	327/141	473	-6.758	16.08	-27.12	258.1	-9.964	67.37	1.051	.450	.2387
.25	12.44	12.84	335/142	327/141	473	-12.07	23.89	-19.42	267.1	-13.52	72.35	1.054	.450	.2464
.28	13.69	13.07	460/187	450/186	777	-16.16	36.98	-9.90	279.2	-17.83	77.76	1.058	.450	.2464
.30	14.53	13.53	622/249	612/248	1278	-19.30	45.05	-2.61	285.6	-21.16	81.61	1.060	.451	.2487

TABLE VIII. — The same as table V for $S/A = 2$.

T	R_c	M/Z	β_{c1}/Zc_1	Γ	P_{max}	μ_n	μ_p	μ_e	P_{eet}	F_{eet}/A	S_{eet}/A	Y_e	
(m^{-2}) (MeV)	(fm)				(MeV m^{-3})	(MeV)	(MeV)	(MeV)	(MeV m^{-3})	(MeV)	(MeV)		
.001	3.13	25.47	107/38	82/34	18	-0.045	-7.96	-14.67	42.3	-0.053	2.43	2.085	.446
.005	4.96	18.20	126/44	96/39	25	-0.073	-8.53	-18.85	72.5	-0.058	10.48	2.090	.456
.01	6.07	14.67	132/46	102/41	27	-0.0919	-8.81	-21.20	91.4	-0.133	15.23	2.080	.455
.02	7.47	12.68	171/60	134/53	43	-0.289	-9.35	-26.57	115.2	-0.2807	21.08	2.083	.455
.03	8.39	11.95	214/75	170/67	64	-0.3832	-9.76	-29.77	131.9	-0.4750	25.18	2.077	.455
.04	9.16	11.71	269/94	218/85	97	-0.5567	-10.15	-32.49	145.2	-0.6905	28.29	2.078	.454
.05	9.76	11.94	358/125	290/113	157	-0.7422	-10.52	-34.75	156.5	-0.9219	30.98	2.076	.454
.065	10.35	10.72	339/117	211/84	91	-0.9825	-11.35	-38.48	170.9	-1.2343	34.61	2.073	.453
.07	9.95	1.02	-11.78	-37.72	175.5	1.301	37.79	2.079	457	1.583			
.08	10.81	1.260	-12.17	-40.29	183.3	1.598	38.31	2.071	454	1.632			
.09	11.63	1.545	-12.27	-42.37	190.5	1.935	38.83	2.073	454	1.632			
.10	12.41	1.872	-11.68	-44.00	197.1	2.314	39.36	2.074	462	1.632			
.11	13.16	2.243	-11.68	-46.02	209.2	2.740	40.85	2.077	451	1.609			
.12	13.89	2.663	-11.00	-46.46	214.7	3.247	41.23	2.079	450	1.937			
.13	14.59	3.134	-10.09	-46.46	214.7	3.747	41.23	2.079	450	1.937			
.14	15.27	3.660	-8.96	-46.54	220.0	4.335	41.96	2.080	450	1.995			
.15	15.93	4.244	-7.62	-46.28	225.0	4.983	42.76	2.081	450	2.046			
.18	17.80	6.376	-2.35	-43.59	238.6	7.323	43.35	2.086	450	2.175			
.20	18.99	8.142	2.09	-40.32	246.9	9.242	47.77	2.088	450	2.243			
.22	20.12	10.21	7.24	-35.97	254.6	11.48	50.27	2.091	451	2.299			
.25	21.74	13.92	16.21	-27.54	265.3	15.46	54.55	2.096	453	2.345			
.28	23.28	18.41	26.56	-16.99	275.1	20.27	59.49	2.100	458	2.415			
.30	24.72	21.87	34.19	-8.86	281.2	23.97	63.12	2.103	468	2.441			

TABLE X. — The same as table I for the force SkM , $S/A = I$ and $Y_e = 0.30$.

T	R_c	M/Z	β_{c1}/Zc_1	Γ	P_{max}	μ_n	μ_p	μ_e	P_{eet}	F_{eet}/A	S_{eet}/A	Y_e		
(m^{-2}) (MeV)	(fm)				(MeV m^{-3})	(MeV)	(MeV)	(MeV)	(MeV m^{-3})	(MeV)	(MeV)			
.001	1.35	31.17	127/38	109/38	43	-0.032	-2.84	-20.81	40.7	-0.033	1.18	1.014	.323	.12
.005	2.59	19.49	160/48	138/48	65	-0.066	-2.97	-23.37	89.6	-0.087	8.21	1.027	.350	.15
.01	3.22	16.62	192/58	167/58	89	-0.085	-2.91	-25.48	97.7	-0.060	12.74	1.029	.358	.16
.02	3.95	14.62	262/79	231/78	153	-0.1654	-2.78	-28.43	110.5	-0.1933	18.46	1.030	.365	.15
.03	4.44	13.94	344/103	304/103	244	-0.2811	-2.71	-30.64	126.5	-0.323	22.46	1.032	.369	.17
.04	4.81	13.94	454/136	403/135	393	-0.4091	-2.63	-32.92	139.2	-0.4649	25.62	1.031	.371	.17
.0														

TABLE XII. — The same as table I for the force $S'I'$, $S/A = 1$ and $Y_e = 0.30$.

T	R_c	R/L	R_{c1}/L_{c1}	Γ	P_{e0}	μ_n	μ_p	μ_α	P_{e0}	F_{e0}/A	S_{e0}/A	Y_e	
(fm^{-3}) (MeV)	(fm)			(MeV)	(MeV fm^{-3})	(MeV)	(MeV)	(MeV)	(MeV fm^{-3})	(MeV)	(MeV)		
.001	1.49	32.34	142/43	120/42	54	.0031	-2.51	-21.01	46.7	.0033	1.33	1.014	.321
.005	2.57	20.55	182/55	155/54	81	.0246	-2.56	-23.86	49.6	.0295	8.23	1.025	.347
.01	3.23	17.42	221/66	192/66	112	.0664	-2.45	-26.23	87.6	.0782	12.65	1.028	.355
.02	4.00	15.36	303/91	268/91	153	.1446	-2.27	-29.56	110.4	.1905	18.20	1.030	.362
.03	4.50	14.75	403/121	361/121	215	.2792	-2.18	-32.03	126.5	.3265	22.10	1.030	.365
.04	4.87	14.71	533/160	482/159	309	.4054	-2.13	-34.05	139.2	.4776	25.19	1.030	.367
.05	5.17	15.01	708/213	645/211	429	.5406	-2.11	-35.82	150.0	.6404	27.79	1.030	.368
.06	5.43	15.39	953/286	873/284	573	.6829	-2.12	-37.42	159.4	.8126	30.04	1.030	.369
.07	5.71	16.67	1358/407	1351/407	833	.9432	-2.12	-39.77	167.8	.9488	31.90	1.030	.369
.08	5.92	15.27	1194/358	883/358	1265	.9439	-2.74	-41.28	175.4	1.1366	33.58	1.030	.370
.09	6.11	14.19	1076/333	582/333	1689	1.044	-2.72	-42.70	182.5	1.3309	35.12	1.029	.370
.10	6.29	13.32	991/297	378/297	246	1.2890	-2.73	-44.06	189.0	1.5304	36.54	1.029	.370
.11	6.46	12.57	915/275	230/275	341	1.4539	-2.77	-45.36	195.1	1.7335	37.86	1.030	.370
.12	6.40					1.496	-3.84	-46.09	200.9	1.844	39.80	1.029	.373
.13	6.76					1.683	-2.18	-46.25	206.3	2.265	40.60	1.029	.372
.14	7.12					2.354	-1.10	-45.79	211.4	2.770	41.51	1.030	.371
.15	7.46					2.937	2.40	-44.71	216.3	3.370	42.54	1.031	.371
.18	8.47					5.261	12.45	-37.78	229.7	5.839	46.43	1.033	.371
.20	9.12					7.468	21.30	-30.05	237.8	8.145	49.75	1.034	.371
.22	9.76					10.28	31.89	-19.84	245.4	11.07	53.69	1.036	.373
.25	10.68					15.82	51.08	0.15	256.0	16.82	60.87	1.039	.376
.28	11.59					23.18	74.25	25.75	285.7	24.44	69.66	1.042	.381
.30	12.18					29.23	91.93	45.93	271.8	30.70	76.46	1.045	.385

TABLE XIII. — Two typical points on the $S/A = 1$, $Y_e = 0.30$ adiabat computed with T6 using different TF approximations (see section 4 for explanation).

T	R_c	N/Z	R_{c1}/L_{c1}	Γ	P_{e0}	μ_n	μ_p	μ_α	P_{e0}	F_{e0}/A	S_{e0}/A	Y_e	
(fm^{-3}) (MeV)	(fm)				(MeV fm^{-3})	(MeV)	(MeV)	(MeV)	(MeV fm^{-3})	(MeV)	(MeV)		
.04	4.56	14.12	471/141	429/141	444	.6055	-1.93	-34.13	139.3	.4768	26.57	1.028	.366
	4.63	14.45	506/152	459/151	493	.6044	-2.04	-33.85	139.2	.4767	25.36	1.028	.367
.08	4.63	13.67	428/128	391/128	372	.4083	-1.85	-34.53	139.2	.4764	25.04	1.029	.365
	5.43	13.76	872/262	612/192	713	.9420	-2.42	-41.28	175.5	1.1324	33.80	1.027	.369
	5.44	14.00	920/276	641/201	774	.9370	-2.51	-41.22	175.5	1.1282	33.65	1.027	.370
	5.46	13.82	865/266	625/195	727	.9458	-2.37	-41.35	175.5	1.1355	33.74	1.028	.369

TABLE XIV. — Plasma effects computed along the $S/A = 1$, $Y_e = 0.30$ adiabat. The force used was T6 (see section 5 for explanation).

F_{e0}/A	P_{e0}	S_{e0}/A	
(MeV fm^{-3}) (MeV)	(MeV fm^{-3})	(MeV fm^{-3})	
.001	-1.02(-1)	1.95(-5)	5.51(-2)
.005	-1.02(-1)	1.72(-4)	3.21(-2)
.01	-9.73(-2)	2.63(-4)	2.42(-2)
.02	-8.01(-2)	4.15(-4)	1.58(-2)
.03	-6.56(-2)	5.27(-4)	1.14(-2)
.04	-5.27(-2)	5.83(-4)	8.36(-3)
.05	-4.13(-2)	5.90(-4)	6.10(-3)
.06	-3.24(-2)	5.66(-4)	4.52(-3)
.07	-2.65(-2)	5.49(-4)	3.55(-3)
.08	-2.38(-2)	7.48(-4)	4.30(-3)
.09	-4.35(-2)	1.01(-3)	5.79(-3)
.10	-6.41(-2)	1.71(-3)	8.42(-3)

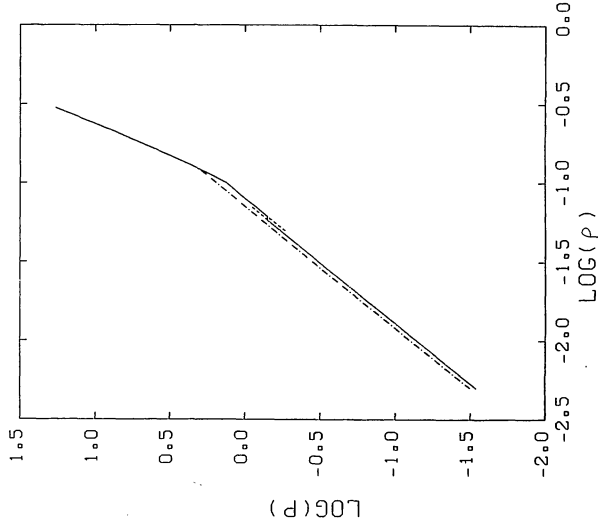


FIGURE 1. — $\text{Log } p$ vs. $\text{log } \rho_B$ for $S/A = 1.5$ and $Y_e = 0.30$. Units are MeV fm^{-3} for p and fm^{-3} for ρ_B .

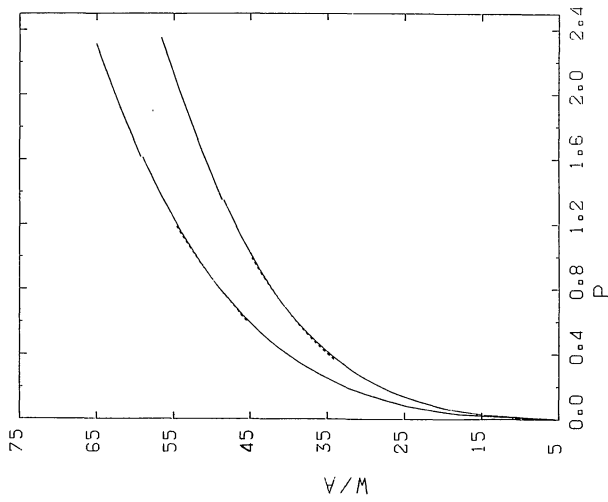


FIGURE 2. — Enthalpy per baryon vs. pressure for $S/A = 1$. The lower curve corresponds to $Y_e = 0.30$ and the other one to $Y_e = 0.35$. Units are MeV for W and MeV fm^{-3} for p . For both curves full lines represent stable and dashed lines metastable EOS pieces.

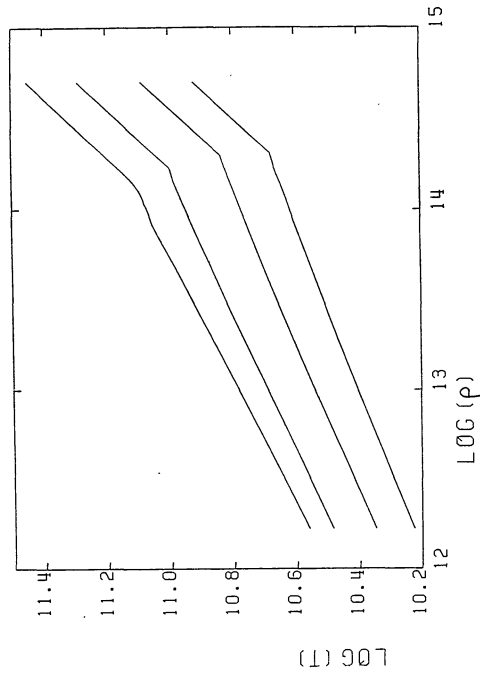


FIGURE 3. — Isentropes for $Y_e = 0.35$. From top to bottom, the isentropes correspond to $S/A = 2, 1.5, 1$ and 0.7 . Units are K for T and $g \text{ cm}^{-3}$ for ρ_B .